TOMOGRAPHY® RESEARCH ARTICLE

Pitfalls in Gallium-68 PSMA PET/CT Interpretation—A Pictorial Review

Deepa Shetty[1], Dhruv Patel[1], Ken Le[1], Chuong Bui[1,2], and Robert Mansberg[1,2]

[1]Department of PET and Nuclear Medicine, Nepean Hospital, Sydney, NSW, Australia; and [2]Nepean Clinical School, University of Sydney, NSW, Australia

Corresponding Author:
Robert Mansberg, MD
Department of PET and Nuclear Medicine, Nepean Hospital, Derby St. Penrith New South Wales, Australia 2751;
E-mail: mansberg@usyd.edu.au

Key Words: Ga 68 PSMA PET/CT, prostate cancer, pitfalls
Abbreviations: Prostate-specific membrane antigen (PSMA), positron emission tomography (PET), computed tomography (CT), [2-hydroxy-5-(carboxyethyl)benzyl] ethylenediamine-diacetic acid (HBED-CC)

ABSTRACT

The novel Gallium-68 prostate-specific membrane antigen (PSMA)-bis [2-hydroxy-5-(carboxyethyl)benzyl] ethylenediamine-diacetic acid positron emission tomography (PET) tracer is increasingly used in the evaluation of prostate cancer, particularly in the detection of recurrent disease. However, PSMA is expressed in non-prostatic tissues, as well as in other pathologic conditions. Here we illustrate such interpretive pitfalls with relevant images that one may encounter while reporting PSMA PET/CT. This study aims to show variation in physiological distribution of PSMA activity and uptake in various benign and neoplastic disorders that may be misinterpreted as prostatic metastatic disease. These pitfalls are illustrated to enhance awareness, aiding a more accurate interpretation of the study. Retrospective database of all (68)Ga PSMA PET/CT was created and reviewed. In total, 1115 PSMA PET/CT studies performed between February 27, 2015, and May 31, 2017, were reviewed. Any unusual uptake of PSMA was documented, described, and followed up. All cases were then subdivided into the following 4 categories: physiological uptake, benign pathological uptake, nonprostatic neoplastic uptake, and miscellaneous uptake. A variety of nonprostatic tissues and lesions, including accessory salivary gland, celiac ganglion, gall bladder, Paget's bone disease, reactive lymph nodes, non–small cell lung cancer, renal cell cancer, and neuroendocrine tumor, were found to show PSMA uptake. PSMA uptake is not prostate-specific and can be taken up physiologically and pathologically in non-prostatic tissue. It is important for reporting physicians to recognize these findings and instigate appropriate investigations when required while avoiding unnecessary procedures in physiological variation.

INTRODUCTION

Morphological imaging methods exhibit considerable limitations: sensitivity ranges between 25% and 54% for detection of local recurrence of prostate cancer by transrectal ultrasonography or computed tomography (CT) and is moderately improved using functional magnetic resonance (MR) imaging techniques (1-3). Gallium-68 prostate-specific membrane antigen (PSMA)-bis [2-hydroxy-5-(carboxyethyl)benzyl] ethylenediamine-diacetic acid (HBED-CC) is a relatively new positron emission tomography (PET) tracer that is increasingly used in the detection of prostatic metastases at staging and in the evaluation of recurrent disease (4-8). Studies suggest that 68-PSMA-ligand PET/CT is fairly sensitive and highly specific in the detection of prostatic metastases even at low prostate-specific antigen levels (7, 9, 10). PSMA is a cell surface protein, with significantly increased expression in prostate cancer cells than in other PSMA-expressing tissues such as kidney, proximal small intestine, and salivary glands (11, 12). Imaging with Gallium-68 PSMA-bis-HBED-CC is based on the fact that it specifically binds to PSMA on the cell membrane of prostatic tumor cells. However, it has been shown that various normal nonprostatic tissues also express PSMA and therefore show PSMA tracer avidity. Some of the PSMA-avid nonprostatic malignancies have also been shown to express PSMA on their cell or in their neovascularity and could be confused with prostatic metastases. The purpose of this review is to illustrate such interpretive pitfalls that one may encounter during reporting by a process of literature review and integrating some of our cases as examples to help avoid misdiagnosis and mismanagement.

METHODOLOGY

A significant number of Gallium-68 PSMA PET/CT are performed at our center (~12–15/week). A database is maintained within the department that comprises deidentified patient information, information pertaining to primary prostate malignancy, stage-defined findings on PSMA PET/CT, and any unusual PSMA uptake. A retrospective observation and a review of consecutive 1115 PSMA PET/CT studies performed between February 27, 2015, and May 31, 2017 were conducted by the authors of this paper.

ISSN 2379-1381 http://dx.doi.org/10.18383/j.tom.2018.00021

PSMA uptake related to prostate carcinoma within the prostate gland, lymph nodes, or metastases was excluded. Any unusual PSMA uptake was documented, described, and followed up. All such cases were then subdivided into the following 4 categories: physiological uptake, benign pathological uptake, nonprostatic neoplastic uptake, and miscellaneous uptake. The images of such cases were downloaded after deidentification via 2 different picture archive and communication system (PACS) software used at our center, that is, general electronics (GE) and MedView PACS. A literature review was performed to identify similar cases reported in the literature and have been cited here.

Tracer Preparation and Imaging Protocol/Technique

Gallium-68 ($^{68}Ga^{3+}$) is obtained using a Germanium-68/Gallium-68 (68Ge/68Ga) radionuclide generator and used for radiolabeling of PSMA-HBED-CC using automated a radiosynthesizer. The labeling efficiency of the radiopharmaceutical is typically >98%. The tracer dose is dependent on the patient's weight: <60 kg, 61–90 kg, and >90 kg, receiving 200 MBq, 250 MBq, and 300 MBq, respectively, in our department and is administered via an intravenous injection. The PET/CT images from skull vertex to knees are acquired at 30 min post injection on a Phillips Gemini TF 64 slice PET/CT camera (Phillips Medical Systems, Cleveland). A concurrent low-dose CT (120 keV and 60 mAs per section) with dilute oral contrast of the same region is also performed for lesion localization and attenuation correction. Emission data are corrected for attenuation, scatter, and decay and these are processed as per the vendor reconstruction protocol. The PET, low-dose CT, and fused PET/CT images are then sent to the workstation for interpretation.

RESULT AND DISCUSSION

General Distribution of PSMA Uptake in The Body

PSMA is an integral membrane protein of the prostatic epithelium with both intracellular and extracellular domain. It has several enzymatic functions such as glutamate-preferring carboxypeptidase. The effect of these enzymatic functions is not understood; however, it has been shown that PSMA does have an internalization signal that allows internalization of the protein on the cell surface into an endosomal compartment (13). PSMA is expressed in both benign and malignant prostate pathologies and is upregulated following androgen deprivation (14, 15). In addition to the prostate, which shows mild diffuse PSMA uptake, various other normal and pathological tissues also take up PSMA tracer related to immunoexpression of PSMA on their cells (16-18). PSMA is expressed in other cancers as well, more specifically in the neovasculature associated with these cancers (17). The degree of PSMA uptake of these tissues is dependent on the extent of PSMA expression. PSMA uptake is mild in pancreatic head, Waldeyer ring, and fossa of Rosenmüller, and moderate in proximal small bowel, liver, and spleen. Marked PSMA tracer activity is seen in kidneys, salivary glands, lacrimal glands, and vocal cords. Intense uptake in renal pelvis, ureters, and urinary bladder is mostly related to excretion (Figure 1). Although PSMA immunoexpression is also established in the brain, heart, urinary bladder, testis, and endometrial glands, the extent of expression is minimal, and therefore, it does not show significant uptake.

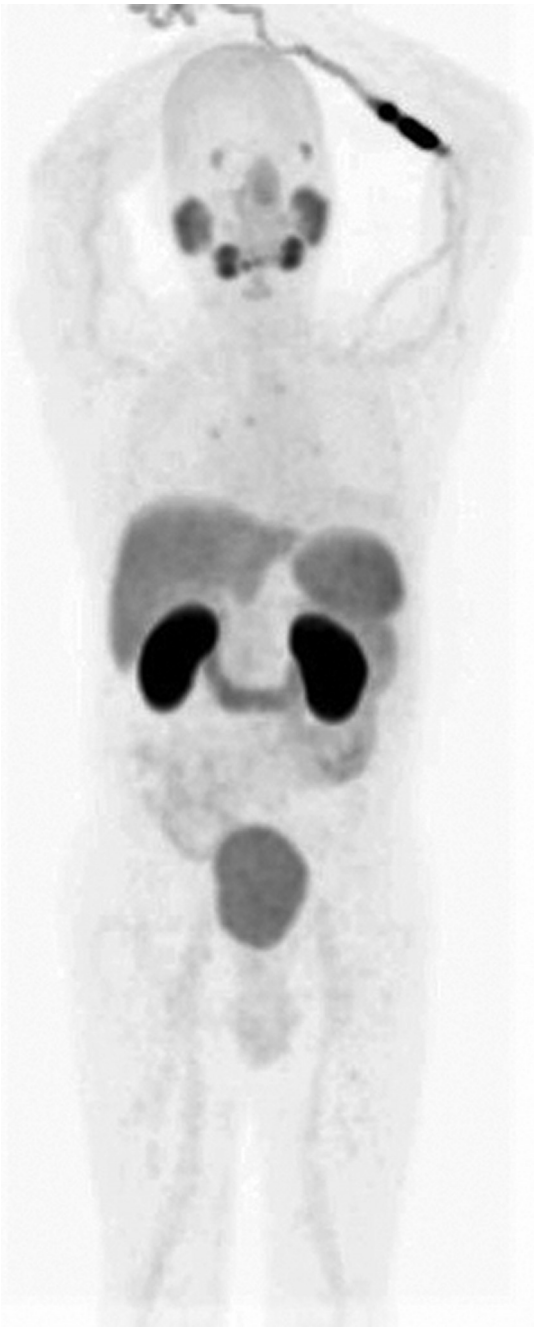

Figure 1. Anterior reprojection emission prostate-specific membrane antigen (PSMA) positron emission tomography (PET) image from skull vertex to knees showing the normal distribution of the PSMA tracer. Intense activity is seen in the kidneys with moderate activity in the lacrimal glands, salivary glands, liver, spleen, proximal small bowel, and urinary bladder. The injection site in the left cubital fossa shows marked activity.

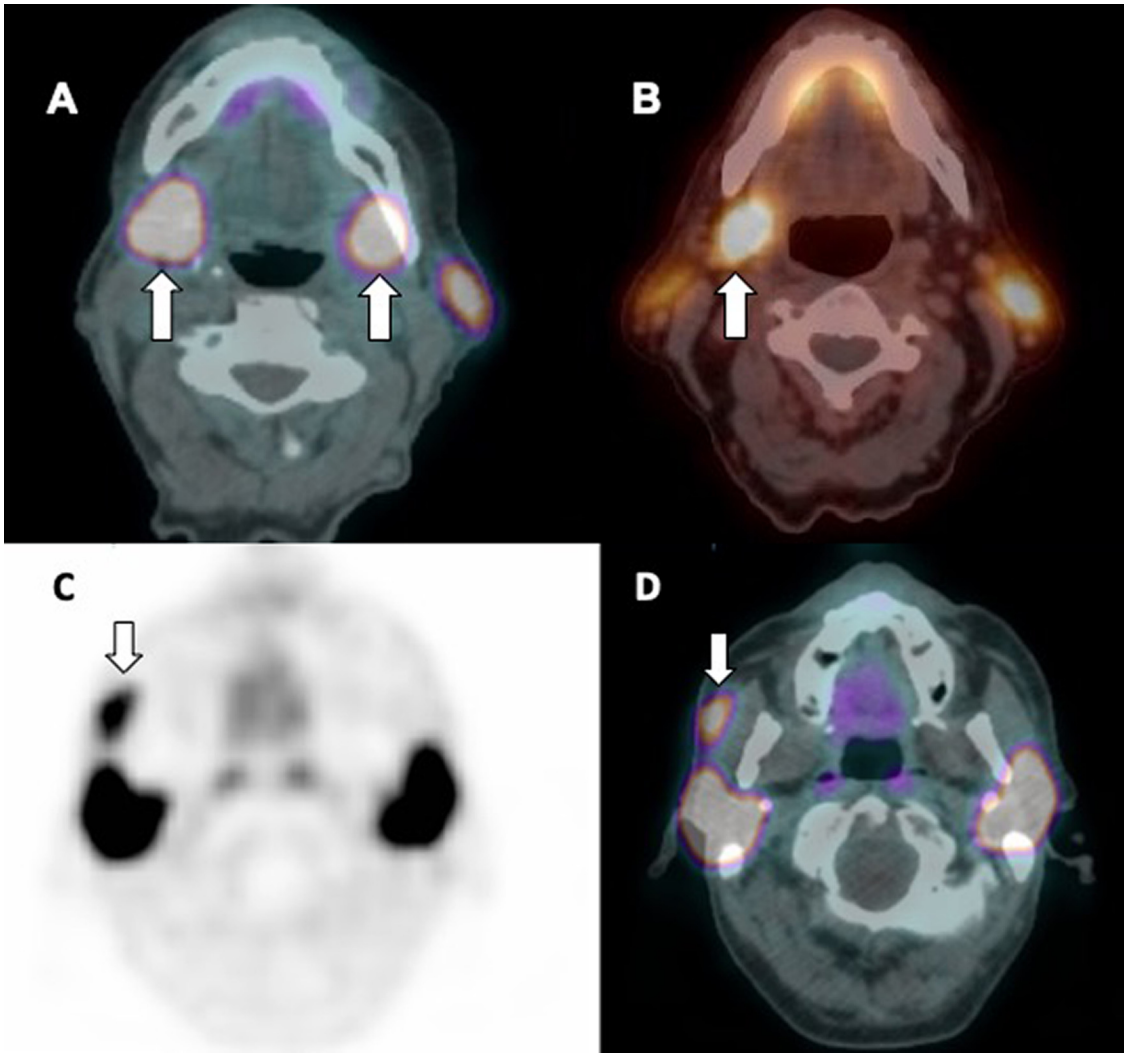

Figure 2. Axial PSMA PET/low-dose computed tomography (CT) fused image showing symmetrical (A) and asymmetrical PSMA (B) uptake in the right submandibular gland, while the left submandibular gland is not visible in a different patient, which may be due to atrophy or agenesis. Axial PSMA PET/CT-fused (C) and CT (D) images showing marked PSMA uptake in the right accessory parotid gland, which is usually located on the masseter muscle. Concurrent low-dose CT image showing a small low-density soft tissue similar in attenuation to the parotid gland.

Variable Physiological Uptake

Activity is seen in the normal salivary glands, for example, parotid and submandibular glands, as well as accessory parotid gland that is similar to the main parotid and other salivary glands. The submandibular glands are usually symmetrical in size; however, there may occasionally be asymmetric PSMA activity that may be misinterpreted as lymphadenopathy (Figure 2). Accessory parotid glands are seen in ~20% of the population; it is located on the masseter muscle, anterior to the main parotid gland and superior to the Stenson duct (19, 20); and it can be either unilateral or bilateral.

Some of the sympathetic chain ganglia have been shown to take up PSMA including celiac and stellate ganglia (21, 22). Celiac ganglion can be identified by CT in ~96% of male patients. They are located anterior to the diaphragmatic crura, over the anterolateral wall of the aorta bilaterally and just caudal to the origin of the celiac artery. The left celiac ganglion is more often identified than the right (89% vs 67%) (23). They appear as linear multilobulated or discoid-shaped structures (Figure 3, A and B). CT attenuation of Celiac ganglia is same as the adjacent adrenal glands on a non-enhanced CT. Celiac ganglia strongly express PSMA on immunohistochemical analysis (22). The stellate ganglion lies anterior to the neck of the first rib and the C7 transverse process, lateral to the C7/T1 vertebral bodies, and superior to the pleural cupola over the lung apex.

A variable degree of diffuse uptake is occasionally seen in the gall bladder, although the gall bladder does not show significant uptake (Figure 3, C and D). This is likely related to the variability of PSMA expression, and more studies are needed to evaluate other potential causes.

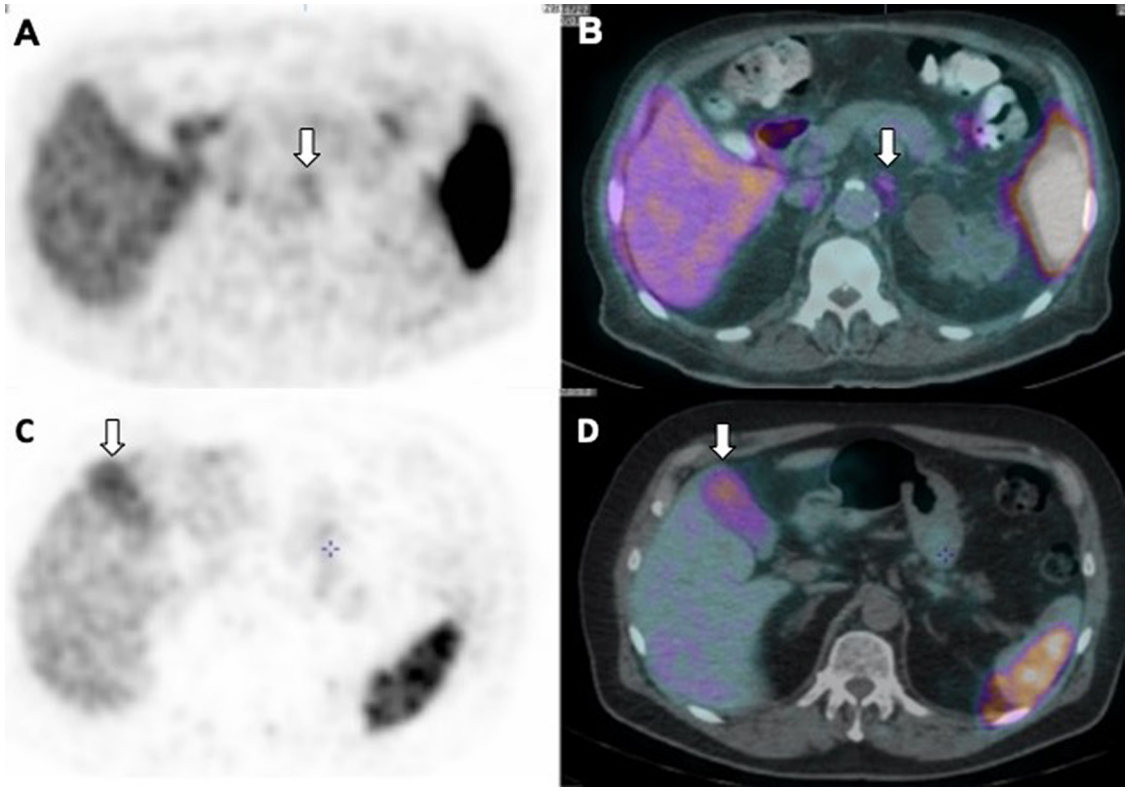

Figure 3. Axial PET image (A) and PET/CT-fused (B) image showing mild uptake in the left celiac ganglion, which appears as an elongated discoid structure anterolateral to the abdominal aorta. Axial PET (C) and PET/CT-fused (D) image showing moderate, diffuse PSMA uptake in the gall bladder, which shows normal configuration on concurrent PET/CT image.

Benign Pathological PSMA Uptake

We encountered foci of PSMA uptake in unusual sites in patients with the magnetic resonance imaging-/biopsy-proven tumor sites in the prostate gland. This may be related to focal prostatitis or areas of benign prostatic hyperplasia as mentioned previously that PSMA is overexpressed to a certain extent in all kinds of prostate pathology, although the degree of expression may be weak. This explains why PSMA may not be suitable in the evaluation of primary tumor.

Mild nonspecific PSMA uptake is not infrequently seen in distant lymph nodes such as axillary or hilar stations in an unusual pattern of metastatic spread, suggestive of reactive etiology (Figure 4). Similar uptake may also be seen in inguinal nodes and may be difficult to entirely exclude metastasis. However, when the uptake is seen in several contiguous lymph node stations, lymphoma or granulomatous disease needs to be considered.

Inflammation and infection may show increased PSMA uptake, thereby mimicking malignancy. We identified PSMA uptake in lung infection/pneumonia, atelectasis, and inflammation related to pleural plaques (asbestos) (Figure 5). Similarly, atherosclerotic arteries show linear diffuse mild PSMA uptake along their walls, which may be related to underlying inflammation.

Diffuse variable PSMA uptake has been reported in Paget disease of the bone (24, 25). Paget disease is a common benign condition in the elderly, affecting ~10% of the population of age >80 years. The various hypotheses to explain the mechanism of uptake include uptake within the neovasculature of the Pagetoid bone and uptake driven by hyperemia and increased radiotracer delivery. Correlation with CT to look for typical appearance of Pagetoid bone including diffuse sclerosis, thickened cortex, bone expansion, and coarsened trabeculae should suggest the right diagnosis (Figure 6).

Similarly, we identified mild focal uptake at sites of healing fractures (Figure 7, A and B). Degenerative arthritis in the spine or peripheral joints may show mild-to-moderate PSMA activity (Figure 7, C–F). This may be misinterpreted as metastatic disease. On the other hand, a possible underlying metastasis in the subchondral aspect of the joint may be overlooked (Figure 8) in the setting of background degenerative arthritis.

A case of mild diffuse bone marrow PSMA uptake in a patient with known polycythemia rubra vera is shown, which has not been previously reported in the literature to the best of our knowledge (Figure 9). Recently, a case of follicular lymphoma showing avid PSMA uptake has been reported (26).

Nonprostatic Neoplastic Conditions

Several nonprostatic neoplasms express PSMA either on their cell membrane or in the endothelial cells of capillary beds of tumor neovasculature and consequently show PSMA uptake (16-18).

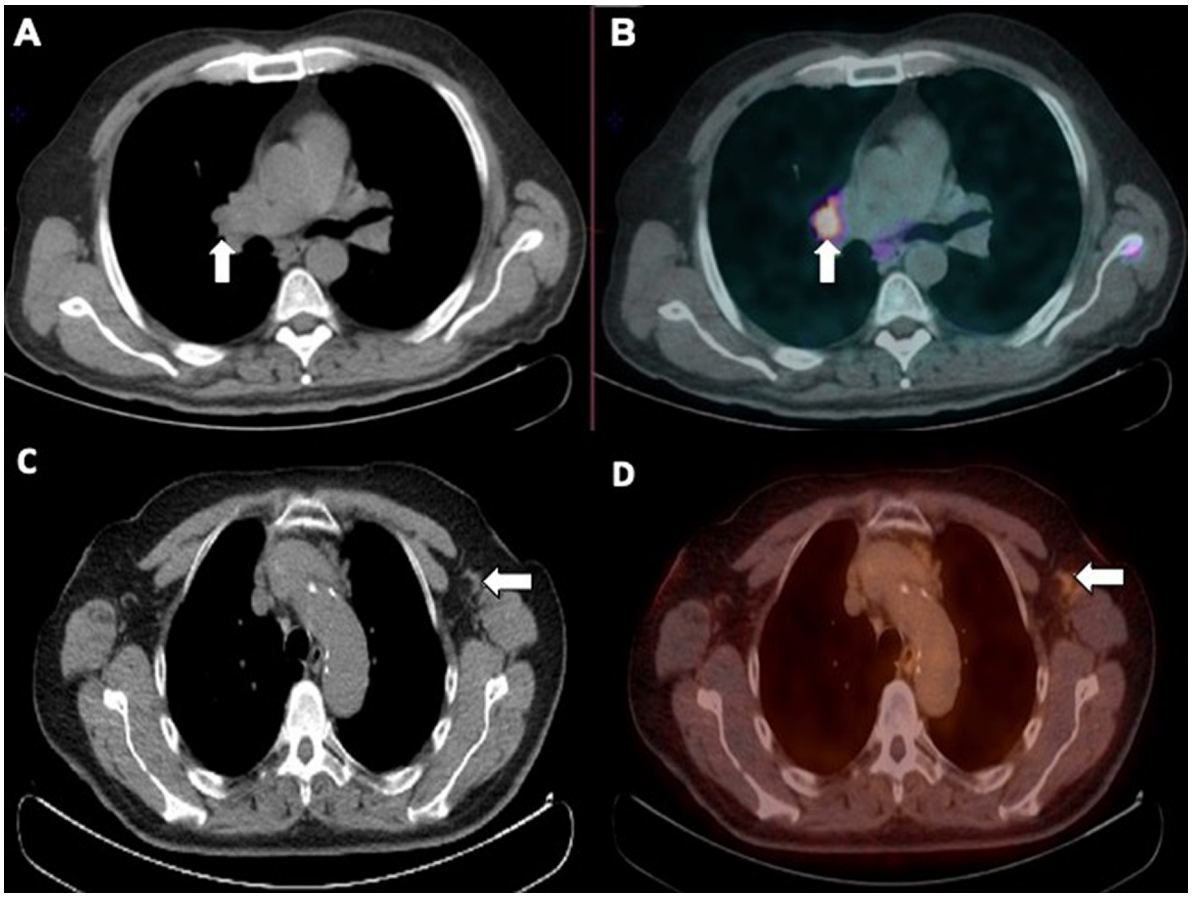

Figure 4. Axial low-dose CT (A) and PET/CT-fused (B) images showing mild uptake at the right pulmonary hilum corresponding to nonenlarged soft tissue/lymph node. Axial low-dose CT (C) and PET/CT-fused (D) images showing mild uptake in a nonenlarged left axillary lymph node.

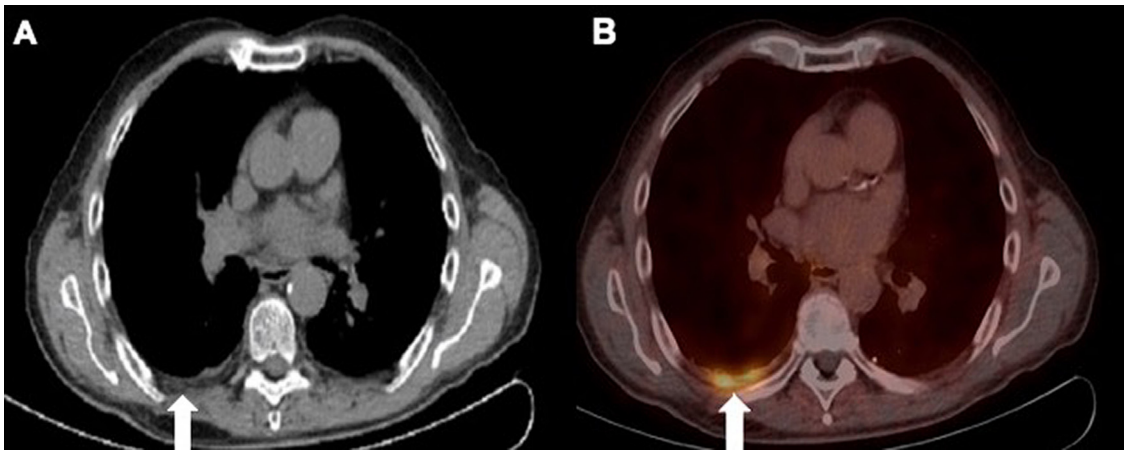

Figure 5. Axial low-dose CT (A) and PET/CT-fused (B) images showing moderate PSMA uptake in the longstanding and stable pleural plaques along the right posterior pleura; the patient had multiple bilateral calcified and noncalcified pleural plaques consistent with the history of asbestos exposure.

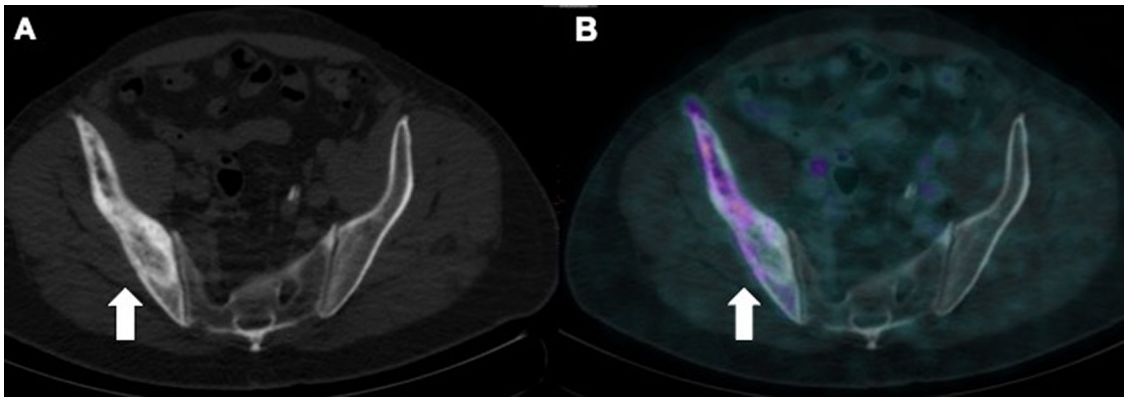

Figure 6. Low dose CT (A) shows Pagetoid changes (thickened cortex, coarsened trabeculae and expanded bone) but mild patchy PSMA uptake is seen in the right ilium on PET/CT (B).

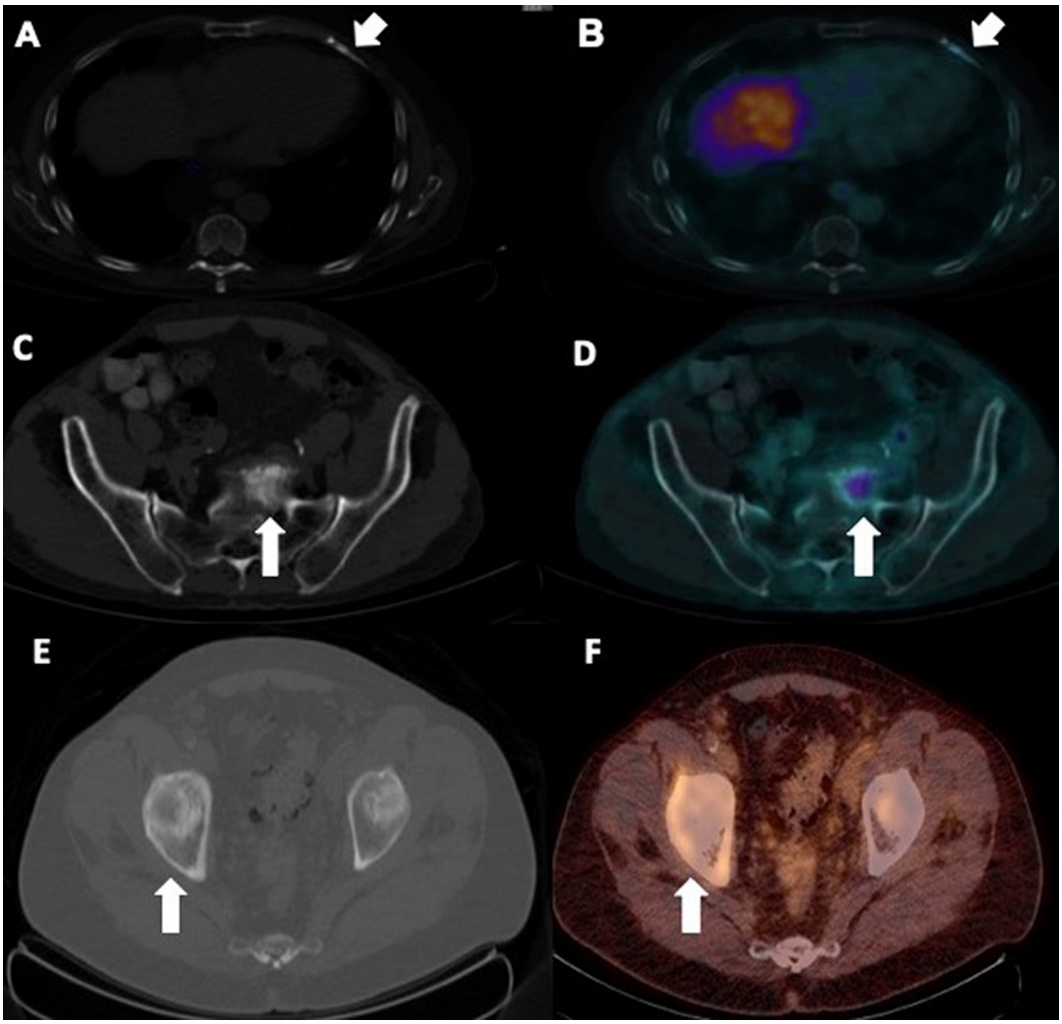

Figure 7. Mild focal PSMA activity at the site of healing fracture in the anterior aspect of the left fifth rib (A and B). Mild diffuse uptake (D) is seen in a large osteophyte lipping of L5/S1 discovertebral joint (C). Osteoarthritic changes in the hips bilaterally (E) show patchy mild PSMA uptake (F).

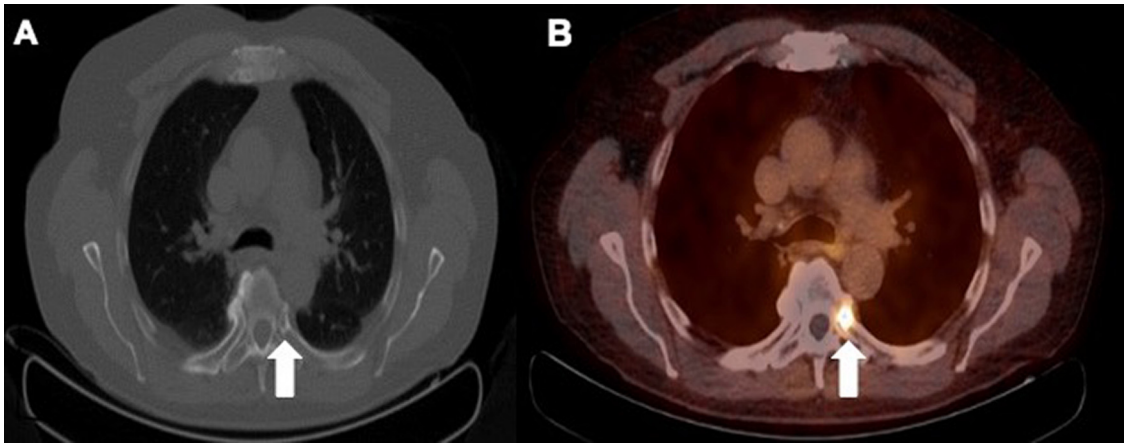

Figure 8. Low-dose CT (A) and PET/CT-fused (B) image showing intense PSMA activity at the costochondral junction corresponding to a small sclerotic focus at the head and neck of the left fifth rib.

PSMA uptake in non–small cell lung cancer with PSMA-avid metastases to the thyroid gland (27) was previously reported by our institution (Figure 10, A and B). Other malignant neoplasms that show PSMA activity include gastric/colonic adenocarcinoma (Figure 10, C–F), renal cell cancer (Figure 11, A and B), neuroendocrine tumor (Figure 11, C and D), gliomas, and breast cancers (17, 27-31). An incidental case of biopsy-proven PSMA-avid hepatocellular carcinoma has been reported by our

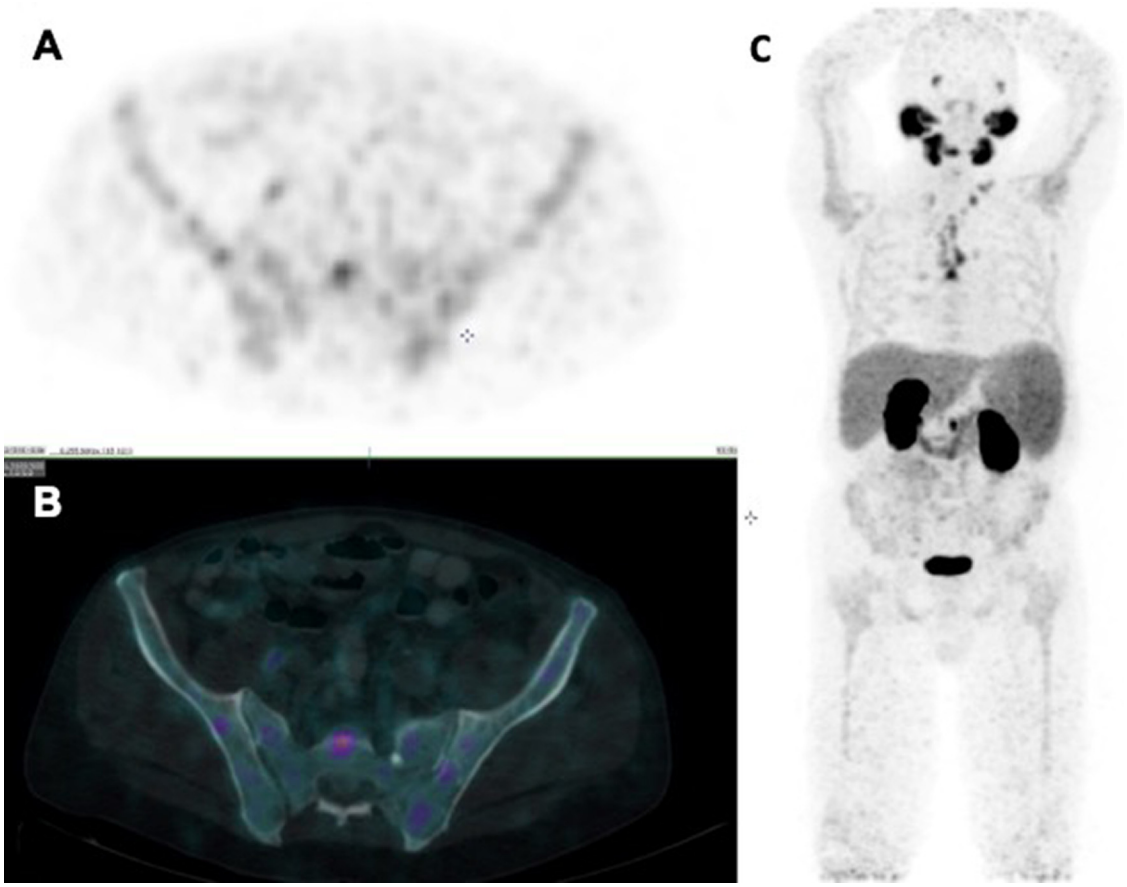

Figure 9. Axial PET (A), PET/CT-fused (B), and anterior reprojection emission PET image (C) showing mild, diffuse PSMA activity in the axial and proximal appendicular skeleton in a patient with known polycythemia rubra vera.

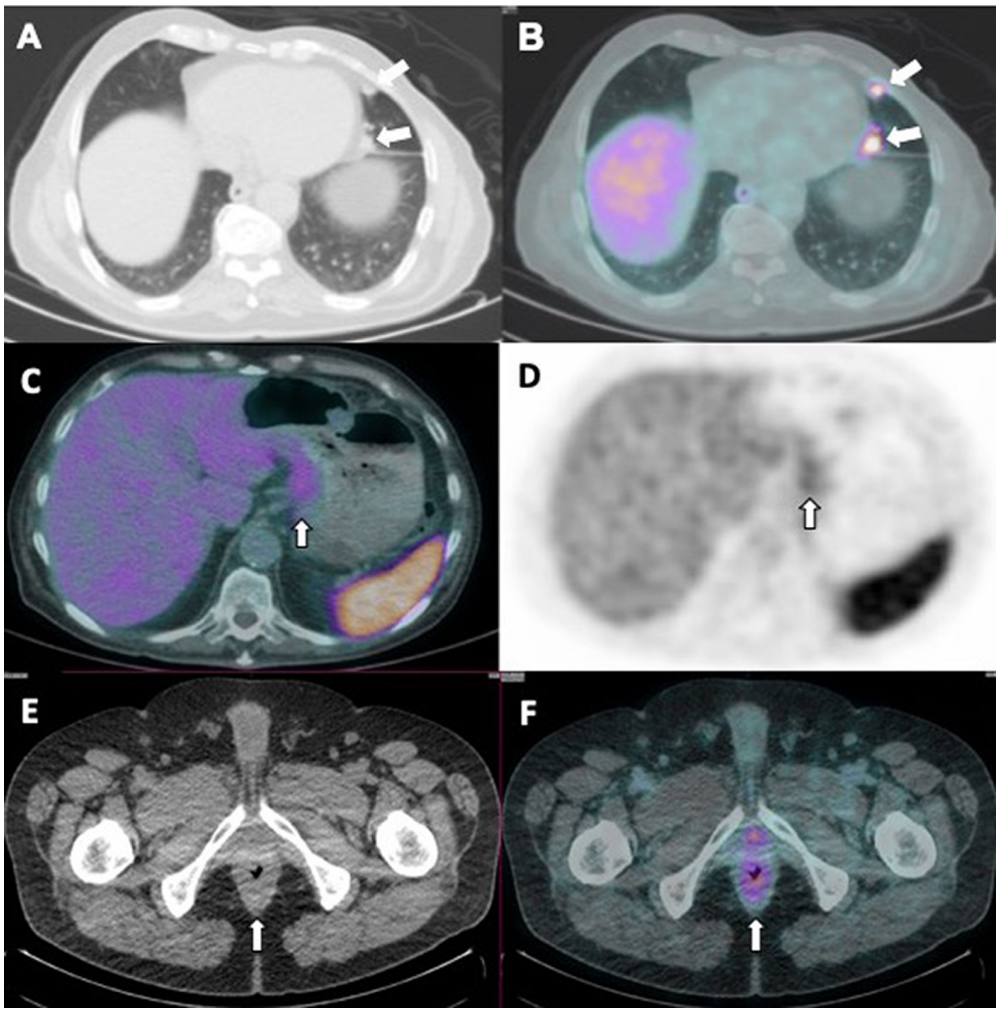

Figure 10. Low-dose CT in lung windows (A) and PET/CT-fused (B) images showing intensely avid PSMA uptake in a case of non–small cell lung cancer recurrence in the lingular lobe. PET/CT-fused (C) and PET (D) images showing mildly increased PSMA uptake in the gastric cardia in a case of high-grade invasive gastric adenocarcinoma. Diffuse rectal wall thickening is shown on a low-dose CT (E) corresponding to mild, diffuse, increased PSMA uptake (F). Further evaluation with biopsy and histopathology assessment revealed a primary rectal malignancy.

institution recently (Figure 12). The PSMA uptake in the endothelium of tumor neoangiogenesis explains the tracer uptake within the tumor.

Benign tumors such as schwannoma and follicular thyroid adenoma have been reported to exhibit PSMA uptake (33-35). PSMA uptake in the thyroid may be because of a differentiated thyroid cancer (34). Evaluation of any PSMA uptake in the thyroid gland (Figure 13) with fine-needle biopsy and histopathological examination is therefore warranted to confirm the underlying pathology.

Miscellaneous PSMA Uptake

Some variants of prostatic carcinoma such as ductal type and cancer with neuroendocrine differentiation may not show significant uptake owing to variation of PSMA expression (36). Sometimes, while the primary focus may be PSMA-positive, the metastases may be PSMA-negative because of heterogeneity of PSMA expression. This may result in false downstaging of the cancer and administration of incorrect treatment. Tissue biopsy and histopathological assessment of the suspected lesion should, in most cases, provide the right diagnosis.

Densely sclerotic and markedly osteoblastic bone lesions found on the bone scan are often very mildly PSMA-avid, indicating small-volume metastases (Figure 14), while subtly sclerotic bone foci on CT can show moderate-to-marked PSMA uptake without significant osteoblastic activity on bone scan.

Mild, diffuse symmetrical uptake was seen in gynecomastia (Figure 15) and the mechanism is not clear considering immunoexpression is not typically identified in the mammary tissue. Other benign unexpected PSMA uptake was also identified in muscles (Figure 16) and cutaneous lesions. Mild PSMA uptake has been noted in atelectasis (Figure 17). Care should be taken to not miss adjacent lung parenchyma, rib, or vertebral body metastases.

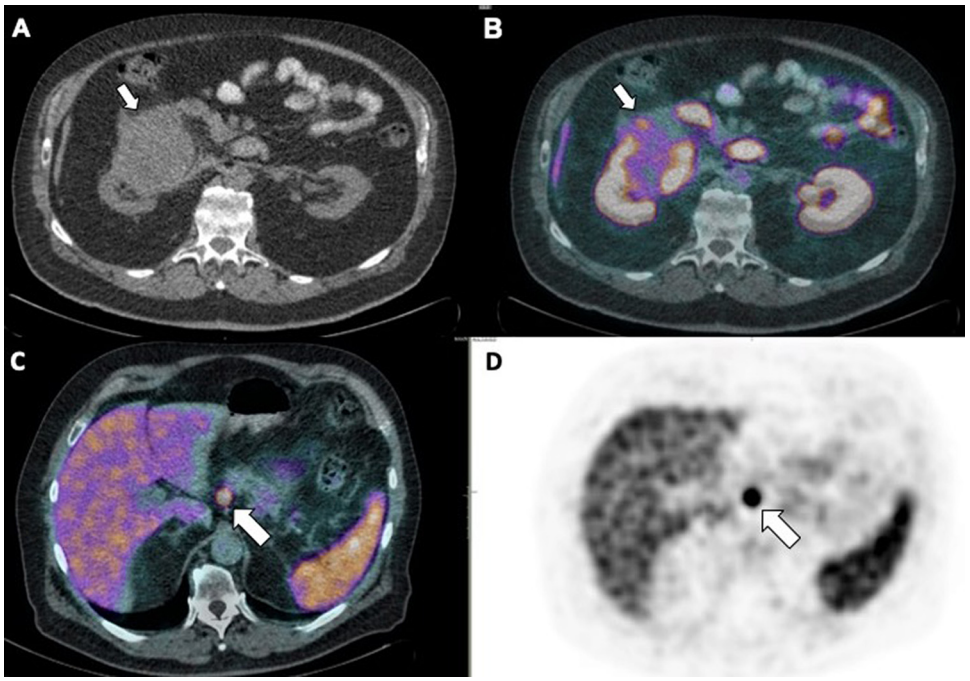

Figure 11. Low-dose CT (A) and fused PET/CT (B) images showing mild heterogeneously increased PSMA uptake in a mass arising from the right kidney that was identified to be renal cell carcinoma after histopathology assessment. An intensely PSMA avid, arterially enhancing pancreatic nodule was incidentally detected during PSMA PET/CT study performed for staging of prostate cancer, as seen in fused PET/CT (C) and PET (D), which was confirmed as neuroendocrine tumour by histopathology.

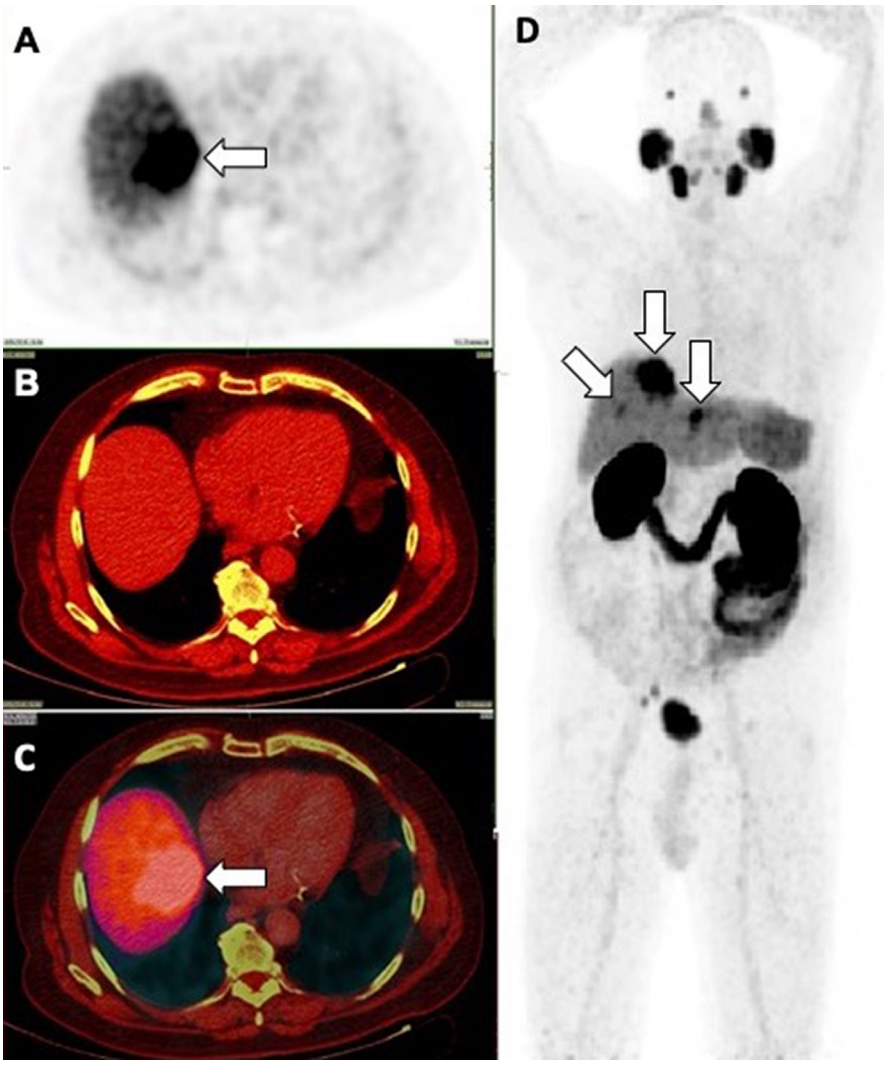

Figure 12. Incidental large, intensely PSMA-avid lesions are seen in the liver, showing arterial enhancement with central washout in venous phase on triple-phase CT as well as magnetic resonance imaging (not shown in the images here). CT-guided core biopsy was performed, and histopathology confirmed well-differentiated hepatocellular carcinoma (A–D) (32).

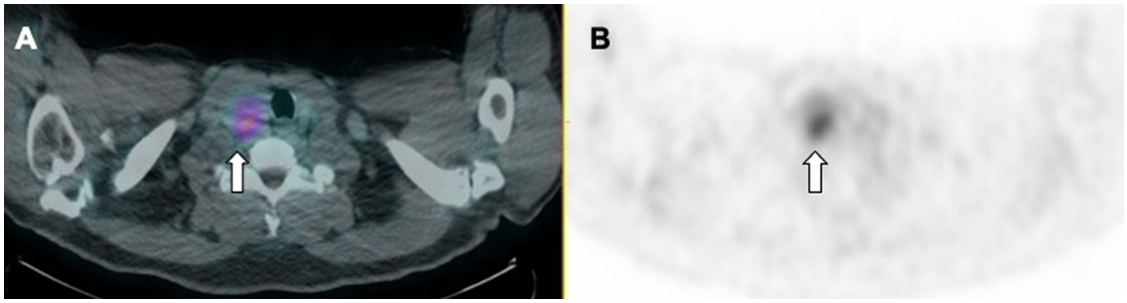

Figure 13. PSMA-PET/CT showing mild-to-moderate increase in nodular uptake in an enlarged right thyroid gland (A–B).

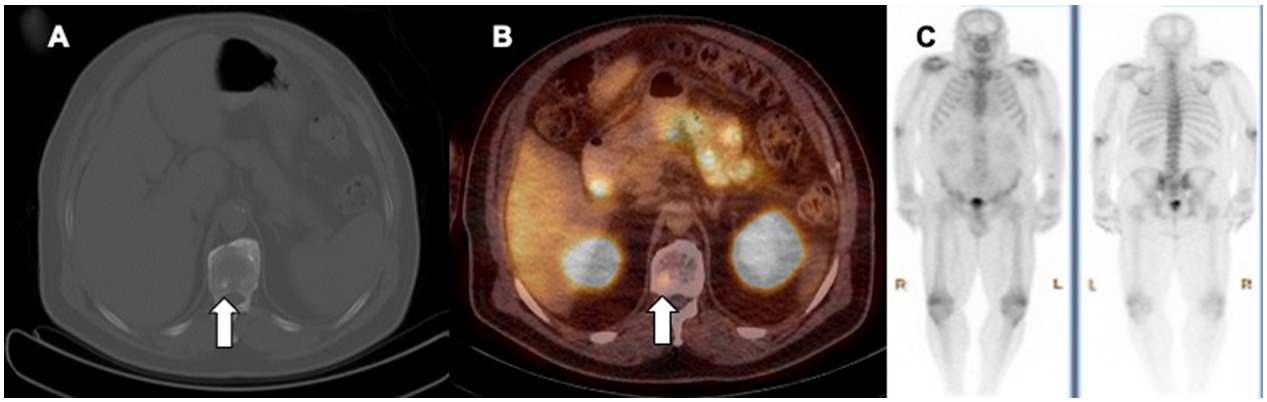

Figure 14. A small mildly sclerotic lesion in the right posterior aspect of the vertebral body was found to be minimally PSMA-avid (A and B) and therefore suspicious for prostatic metastases; however, no corresponding osteoblastic activity on bone scan was identified in the lesion (C).

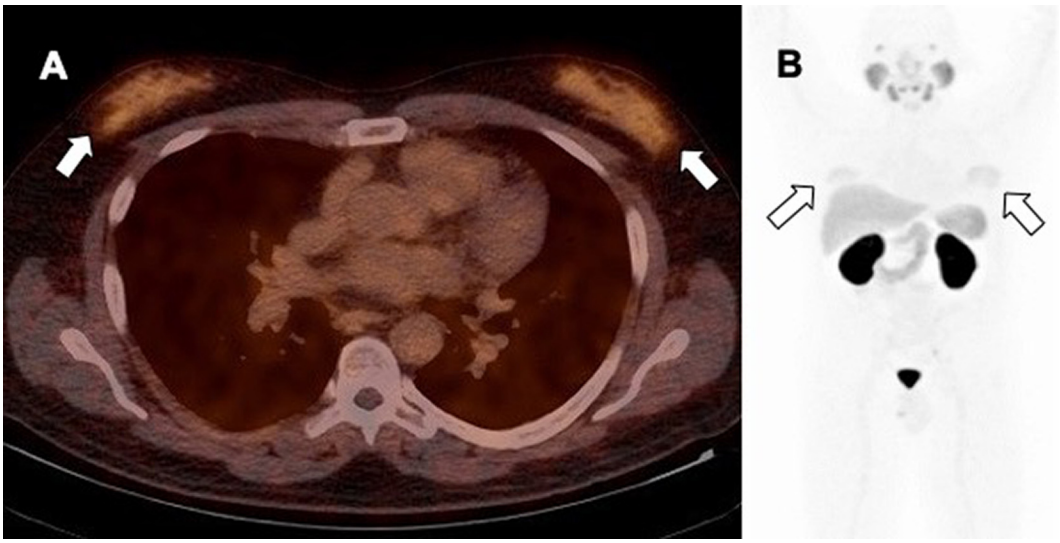

Figure 15. Fused PET/CT (A) and anterior maximum intensity projection image (B) in a gynecomastia demonstrate increased PSMA uptake, thought to be related to antiandrogen therapy for prostate cancer demonstrates mild diffuse symmetrical PSMA activity.

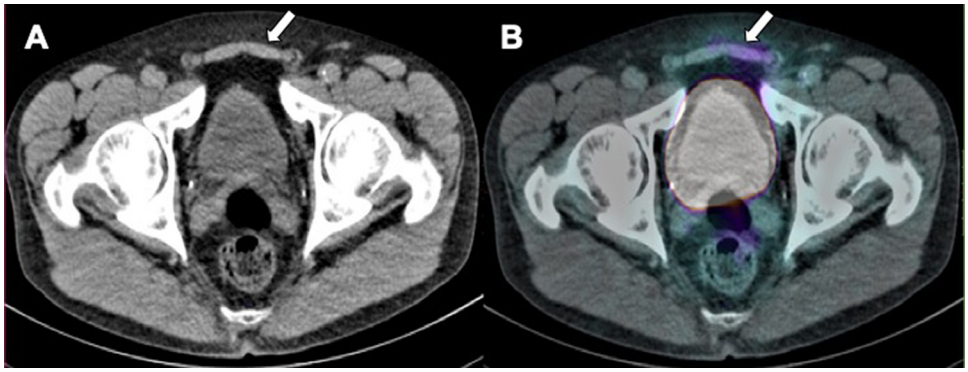

Figure 16. Low-dose CT (A) does not demonstrate any abnormality, at the location of mild asymmetrical PSMA uptake detected in the lower portion of the rectus abdominis (B) likely related to physical activity/trauma.

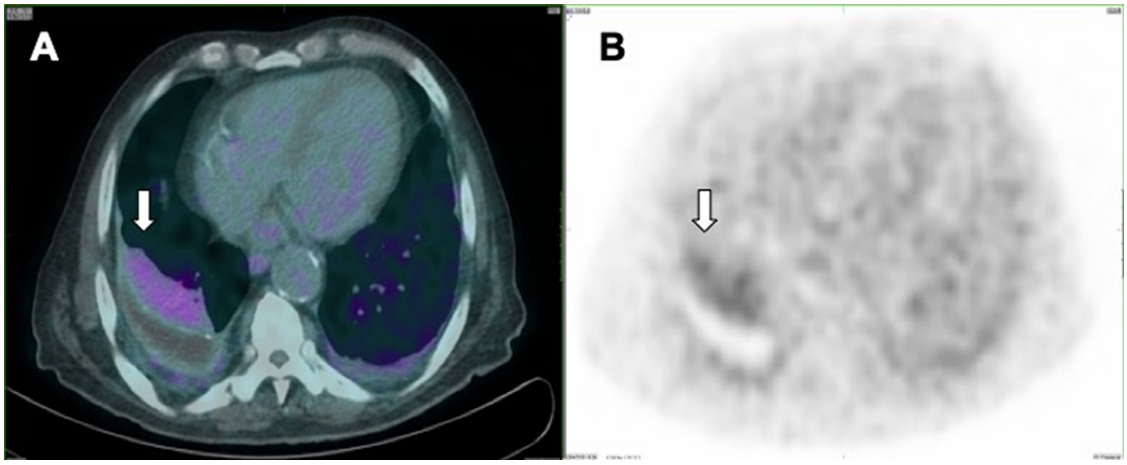

Figure 17. Fused PET/CT (A) and PET (B) demonstrate atelectasis of the right posterior lung base showing PSMA activity. There is absent uptake at the location of a small right effusion. Faint PSMA activity is also noted at mild atelectasis and and pleural thickening along the posterior and lateral aspect of the left hemithorax (A and B).

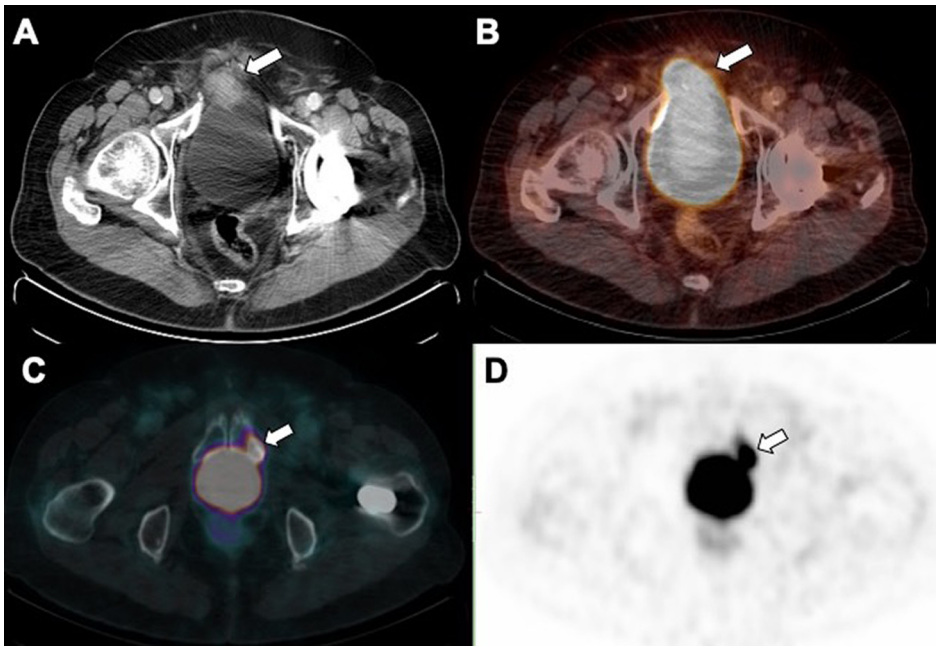

Figure 18. Low dose CT (A) and fused PET/CT (B) show intense activity in the urinary bladder can mask a PSMA avid soft-tissue mass adjacent to the right anterolateral aspect of the urinary bladder which invades the bladder wall. Fused PET/CT (C) and PET (D) demonstrate another example of a PSMA avid sclerotic lesion which can be missed during the initial review due to adjacent PSMA urinary activity in the urinary bladder.

Particular attention needs to be given to the areas adjacent to high physiological PSMA activity, which may be easily overlooked. This can occur particularly around the urinary bladder (Figure 18).

CONCLUSION

As 68Ga-PSMA-ligand PET/CT becomes a more widely used tool in the management of prostate cancer, knowledge of normal physiological distribution, variation in physiological distribution, and confounding PSMA uptake in nonprostatic pathologies is essential to optimize interpretation. Failure to recognize these aspects could result in significant false upstaging or false downstaging and consequent implementation of incorrect management. With newer pathologies being continuously identified to take up PSMA tracer, ongoing learning remains essential. Further studies are required to not only understand the mechanism of PSMA tracer uptake in various other tissues but also establish the potential benefit of PSMA tracer in evaluation of nonprostatic cancers such as fluorodeoxyglucose-negative renal cell carcinoma.

Disclosures: No disclosures to report.

Conflict of Interest: The authors have no conflict of interest to declare.

REFERENCES

1. Beer AJ, Eiber M, Souvatzoglou M, Schwaiger M, Krause BJ. Radionuclide and hybrid imaging of recurrent prostate cancer. Lancet Oncol. 2011;12:181–191.
2. Bott SR. Management of recurrent disease after radical prostatectomy. Prostate Cancer Prostatic Dis. 2004;7:211–216.
3. Castellucci P, Picchio M. 11C-choline PET/CT and PSA kinetics. Eur J Nucl Med Mol Imaging. 2013;40 *Suppl* 1:S36–S40.
4. Afshar-Oromieh A1, Malcher A, Eder M, Eisenhut M, Linhart HG, Hadaschik BA, Holland-Letz T, Giesel FL, Kratochwil C, Haufe S, Haberkorn U, Zechmann CM. PET imaging with a [68Ga]gallium-labelled PSMA ligand for the diagnosis of prostate cancer: biodistribution in humans and first evaluation of tumour lesions. Eur J Nucl Med Mol Imaging. 2013;40:486–495.
5. Jadvar H. Molecular imaging of prostate cancer with PET. J Nucl Med. 2013;54: 1685–1688.
6. Roethke MC, Kuru TH, Afshar-Oromieh A, Schlemmer HP, Hadaschik BA, Fenchel M. Hybrid positron emission tomography-magnetic resonance imaging with gallium 68 prostate-specific membrane antigen tracer: a next step for imaging of recurrent prostate cancer-preliminary results. Eur Urol. 2013;64:862–864.
7. Afshar-Oromieh A1, Avtzi E, Giesel FL, Holland-Letz T, Linhart HG, Eder M, Eisenhut M, Boxler S, Hadaschik BA, Kratochwil C, Weichert W, Kopka K, Debus J, Haberkorn U. The diagnostic value of PET/CT imaging with the (68)Ga-labelled PSMA ligand HBED-CC in the diagnosis of recurrent prostate cancer. Eur J Nucl Med Mol Imaging. 2015;42:197–209.
8. Hofman MS, Iravani A. Gallium-68 prostate-specific membrane antigen PET imaging. PET Clin. 2017;12:219–234.
9. Eiber M, Maurer T, Souvatzoglou M, Beer AJ, Ruffani A, Haller B, Graner FP, Kübler H, Haberkorn U, Eisenhut M, Wester HJ, Gschwend JE, Schwaiger M. Evaluation of hybrid (6)(8)Ga-PSMA ligand PET/CT in 248 patients with biochemical recurrence after radical prostatectomy. J Nucl Med. 2015;56:668–674.
10. Mease RC, Foss CA, Pomper MG. PET imaging in prostate cancer: focus on prostate-specific membrane antigen. Curr Top Med Chem. 2013;13:951–962.
11. Mannweiler S, Amersdorfer P, Trajanoski S, Terrett JA, King D, Mehes G. Heterogeneity of prostate-specific membrane antigen (PSMA) expression in prostate carcinoma with distant metastasis. Pathol Oncol Res. 2009;15:167–172.
12. Sweat SD, Pacelli A, Murphy GP, Bostwick DG. Prostate-specific membrane antigen expression is greatest in prostate adenocarcinoma and lymph node metastases. Urology. 1998;52:637–640.
13. Rajasekaran SA1, Anilkumar G, Oshima E, Bowie JU, Liu H, Heston W, Bander NH, Rajasekaran AK. A novel cytoplasmic tail MXXXL motif mediates the internalization of prostate-specific membrane antigen. Mol Biol Cell. 2003;14:4835–4845.
14. Meller B, Bremmer F, Sahlmann CO, Hijazi S, Bouter C, Trojan L, Meller J, Thelen P. Alterations in androgen deprivation enhanced prostate-specific membrane antigen (PSMA) expression in prostate cancer cells as a target for diagnostics and therapy. EJNMMI Res. 2015;5:66.
15. Wright GL Jr1, Grob BM, Haley C, Grossman K, Newhall K, Petrylak D, Troyer J, Konchuba A, Schellhammer PF, Moriarty R. Upregulation of prostate-specific membrane antigen after androgen-deprivation therapy. Urology. 1996;48:326–334.
16. Silver DA, Pellicer I, Fair WR, Heston WD, Cordon-Cardo C. Prostate-specific membrane antigen expression in normal and malignant human tissues. Clin Cancer Res. 1997;3:81–85.
17. Liu H, Moy P, Kim S, Xia Y, Rajasekaran A, Navarro V, Knudsen B, Bander NH. Monoclonal antibodies to the extracellular domain of prostate-specific membrane antigen also react with tumor vascular endothelium. Cancer Res. 1997;57: 3629–3634.
18. Kirchner J, Schaarschmidt BM, Sawicki LM, Heusch P, Hautzel H, Ermert J, Rabenalt R, Antoch G, Buchbender C. Evaluation of practical interpretation hurdles in 68Ga-PSMA PET/CT in 55 patients: physiological tracer distribution and incidental tracer uptake. Clin Nucl Med. 2017;42:e322–e327.
19. Thoeny HC. Imaging of salivary gland tumours. Cancer Imaging. 2007;7:52–62.
20. Rastogi R, Bhargava S, Mallarajapatna GJ, Singh SK. Pictorial essay: salivary gland imaging. Indian J Radiol Imaging. 2012;22:325–333.
21. Kanthan GL, Hsiao E, Vu D, Schembri GP. Uptake in sympathetic ganglia on 68 Ga-PSMA-HBED PET/CT: A potential pitfall in scan interpretation. J Med Imaging Radiat Oncol. 2017;61:732–738.
22. Krohn T, Verburg FA, Pufe T, Neuhuber W, Vogg A, Heinzel A, Mottaghy FM, Behrendt FF. [(68)Ga]PSMA-HBED uptake mimicking lymph node metastasis in coeliac ganglia: an important pitfall in clinical practice. Eur J Nucl Med Mol Imaging. 2015;42:210–214.
23. Wang ZJ, Webb EM, Westphalen AC, Coakley FV, Yeh BM. Multi-detector row computed tomographic appearance of celiac ganglia. J Comput Assist Tomogr. 2010;34:343–347.
24. Sasikumar A, Joy A, Nanabala R, Pillai MR, T AH. 68Ga-PSMA PET/CT false-positive tracer uptake in Paget disease. Clin Nucl Med. 2016;41:e454–e455.
25. Bourgeois S, Gykiere P, Goethals L, Everaert H, De Geeter FW. Aspecific uptake of 68GA-PSMA in Paget disease of the bone. Clin Nucl Med. 2016;41:877–878.
26. Kanthan GL, Coyle L, Kneebone A, Schembri GP, Hsiao E. Follicular lymphoma showing avid uptake on 68Ga PSMA-HBED-CC PET/CT. Clin Nucl Med. 2016; 41:500–501.
27. Shetty D, Loh H, Bui C, Mansberg R, Stevanovic A. Elevated 68Ga prostate-specific membrane antigen activity in metastatic non-small cell lung cancer. Clin Nucl Med. 2016;41:414–416.
28. Haffner MC, Kronberger IE, Ross JS, Sheehan CE, Zitt M, Mühlmann G, Ofner D, Zelger B, Ensinger C, Yang XJ, Geley S, Margreiter R, Bander NH. Prostate-specific membrane antigen expression in the neovasculature of gastric and colorectal cancers. Hum Pathol. 2009;40:1754–1761.
29. Baccala A, Sercia L, Li J, Heston W, Zhou M. Expression of prostate-specific membrane antigen in tumor-associated neovasculature of renal neoplasms. Urology. 2007;70:385–390.
30. Vamadevan S, Shetty D, Le K, Bui C, Mansberg R, Loh H. Prostate-specific membrane antigen (PSMA) avid pancreatic neuroendocrine tumor. Clin Nucl Med. 2016;41:804–806.
31. Wernicke AG 1, Varma S, Greenwood EA, Christos PJ, Chao KS, Liu H, Bander NH, Shin SJ. Prostate-specific membrane antigen expression in tumor-associated vasculature of breast cancers. APMIS. 2014;122:482–489.
32. Patel D, Loh H, Le K, Stevanovic A, Mansberg R. Incidental detection of hepatocellular carcinoma on 68Ga-labeled prostate-specific membrane antigen PET/CT. Clin Nucl Med. 2017;42:881–884.
33. Wang W, Tavora F, Sharma R, Eisenberger M, Netto GJ. PSMA expression in Schwannoma: a potential clinical mimicker of metastatic prostate carcinoma. Urol Oncol. 2009;27:525–528.
34. Sager S, Vatankulu B, Uslu L, Sonmezoglu K. Incidental detection of follicular thyroid carcinoma in 68Ga-PSMA PET/CT imaging. J Nucl Med Technol. 2016;44: 199–200.
35. Kanthan GL, Drummond J, Schembri GP, Izard MA, Hsiao E. Follicular thyroid adenoma showing avid uptake on 68Ga PSMA-HBED-CC PET/CT. Clin Nucl Med. 2016;41:331–332.
36. Parimi V, Goyal R, Poropatich K, Yang XJ. Neuroendocrine differentiation of prostate cancer: a review. Am J Clin Exp Urol. 2014;2:273–285.